LA-UR- 09-03452

Approved for public release; distribution is unlimited.

Title: A MIMETIC FINITE DIFFERENCE METHOD FOR THE STOKES PROBLEM WITH SELECTED EDGE BUBBLES

Author(s): L. BEIRAO DA VEIGA
K. LIPNIKOV

Intended for: MEETING:
THE MATHEMATICS OF FINITE ELEMENTS AND APPLICATION

Los Alamos
NATIONAL LABORATORY
EST. 1943

A Mimetic Finite Difference method for the Stokes problem with selected edge bubbles

L. Beirão da Veiga * K. Lipnikov †

Abstract

A new mimetic finite difference method for the Stokes problem is proposed and analyzed. The unstable $P_1 - P_0$ discretization is stabilized by adding a small number of bubble functions to selected mesh edges. A simple strategy for selecting such edges is proposed and verified with numerical experiments.

1 Introduction

The discretizations schemes for Stokes and Navier-Stokes equations must satisfy the celebrated *inf-sup* (or the LBB) stability condition [2, 12]. The stability condition implies a balance between discrete spaces for velocity and pressure. In finite elements, this balance is frequently achieved by adding bubble functions to the velocity space. The goal of this article is to show that the stabilizing edge bubble functions can be added only to a small set of mesh edges. This results in a smaller algebraic system and potentially in a faster calculations. We employ the mimetic finite difference (MFD) discretization technique that works for general polyhedral meshes and can accomodate non-uniform distribution of stabilizing bubbles.

The MFD method has been successfully employed for solving problems of continuum mechanics [29], electromagnetics [24], gas dynamics [16], and linear diffusion (see e.g. [25, 26, 14, 23, 5] and references therein). A modern convergence analysis of the MFD methods has been developed in [13] and later in [7, 11, 5, 27]. This analysis resulted in new algebraic methods for building elemental mass [15, 14] and stiffness [11] matrices on arbitrary-shaped elements for a linear diffusion problem. Later these algebraic methods have been developed for higher order MFD methods [23, 8, 5] and the Stokes problem [4, 6]. A-posteriori error estimators have been proposed in [3, 8] for the diffusion problem.

The MFD method shows strong connections with other compatible discretization methods. Connection with the mixed finite method for diffusion problems has been exploited in [9, 10] to develop the first convergence analysis of the MFD method. More recently, the connection between the MFD method and the mixed and hybrid finite volume methods of [19, 20, 22], has been investigated in [21] and a unified formulation has been proposed. For completeness of exposition, we also mention the new class of discrete duality finite volume

*Dipartimento di Matematica F. Enriques, Università degli Studi di Milano, via Saldini 50, 20133 Milano, Italy, *lourenco.beirao@unimi.it*.

†Los Alamos National Laboratory, Theoretical Division, MS B284, Los Alamos, NM, 87545 *lipnikov@lanl.gov*.

(DDFV) methods [18] that, like the MFD methods, are based on a discrete version of the duality relation between the divergence and gradient operators [1, 17].

Flexibility of the mimetic discretization machinery allows to develop MFD methods adjusted to application demands. For instance, by introducing multiple flux unknowns per mesh faces and enforcing a special sparcity structure for elemental mass matrices allowed us to develop and analyze MFD methods with a local flux stencil [27]. These methods are certainly related to multi-point flux approximation (MPFA) finite volume methods. In this article, flexibility of the MFD method is used to tackle the stability problem. The starting point is the formulation of [4], where edge-based degrees of freedom (bubbles) are added to every edge. Here, the bubbles are instead added to the discretization only where needed, therefore yielding a more efficient method. In order to determine where the bubbles are needed, we extend the macroelement methodology [30] to polygonal meshes and introduce a macroelement partition of mesh which (1) can be applied to a very general range of meshes and (2) for which we are able to prove stability of the discrete problem. For instance, edge bubbles need to be added only to every fourth edge of a square mesh, and they are not needed at all on a Voronoi-type mesh.

The paper outline is as follows. In Section 2, we formulate the Stokes problem. In Section 3, we present briefly the MFD method with non-uniform distribution of edge bubbles, formulate mesh requirements and summarize error estimates. In Section 4, the general macroelement stability analysis, developed originally for simplicial meshes, is revisited for polygonal meshes. In Section 5, the macroelement analysis is developed for the MFD method and a simple algorithm for adding stabilizing bubbles is formulated. In Section 6, convergence of the new MFD method is verified with numerical experiments on polygonal and quadrilateral meshes.

2 The Stokes problem

Let Ω be a polygonal domain in $\mathbb{R}^2$. We consider the variational formulation of the Stokes problem with homogeneous Dirichlet boundary conditions:

Find $u \in (H_0^1(\Omega))^2$ and $p \in L_0^2(\Omega)$ such that

$$\begin{cases} \mathcal{A}(\mathbf{u},\mathbf{v}) - \mathcal{B}(\mathbf{v},p) = f(\mathbf{v}) & \forall \mathbf{v} \in (H_0^1(\Omega))^2, \\ \mathcal{B}(\mathbf{u},q) = 0 & \forall q \in L_0^2(\Omega)\ , \end{cases} \tag{1}$$

where the bilinear forms

$$\mathcal{A}(\mathbf{u},\mathbf{v}) = \int_\Omega \mathcal{C}\nabla\mathbf{u} : \nabla\mathbf{v}\, dx \qquad \text{and} \qquad \mathcal{B}(\mathbf{v},p) = \int_\Omega \mathrm{div}(\mathbf{v})\, p\, dx, \tag{2}$$

and $\mathcal{C}$ is a symmetric and positive definite fourth order tensor with components in $L^\infty(\Omega)$.

Above, $H_0^1(\Omega)$ indicates as usual the Sobolev space of order 1 with homogeneous Dirichlet boundary conditions and $L_0^2(\Omega)$ the space of square Lebesgue integrable functions with zero average. Note that everything that follows applies immediately to more general boundary conditions.

Remark 2.1 *The gradient operator ∇ is chosen only for simplicity of exposition and it can be substituted with the symmetric gradient $\varepsilon(\mathbf{u}) = \frac{1}{2}[\nabla(\mathbf{u}) + \nabla^T(\mathbf{u})]$. Everything that follows still holds up to a simple modification of the involved norms.*

3 The MFD method

Our starting point is the mimetic finite difference (MFD) method introduced in [4, 5]. Let Ω_h be a partition of Ω into polygons E. We assume that this partition is conformal, i.e. intersection of two different elements is either a few mesh points, or a few mesh edges (two adjacent elements may share more than one edge), or empty. We allow Ω_h to contain non-convex and degenerate elements.

In the following, we indicate with h_E the diameter of element E, with ∂E the set of its edges, with $|E|$ its area, and with $\mathbf{n}_E^e$ the outward unit normal to edge $e \in \partial E$. Moreover, we set h as the maximum of all h_E, $E \in \Omega_h$. For each edge e, we indicate with h_e its length $|e|$ and with $\mathbf{n}_e$ the outward unit normal fixed once and for all. Let $\mathcal{E}_h$ be the set of all internal edges of Ω_h and $\mathcal{N}$ be the set of all internal vertexes. Finally, we make the following mesh regularity assumptions.

(M1) Each polygon in Ω_h has at most $\bar{N}$ mesh edges, where $\bar{N}$ is independent of h.

(M2) Each polygon E in Ω_h is star shaped with respect to a point $x_E \in E$.

(M3) For each element $E \in \Omega_h$, we connect its verteces with x_E to generate a conformal triangular mesh in Ω_h. We assume that all such triangles are uniformly shape regular, i.e. there exists $\rho > 0$ independent of h such that the radius of the largest inscribed sphere inside each triangle is larger than ρ times the diameter of the triangle.

The auxiliary triangular partition is introduced only for analysis and is not needed in practice. Note that assumptions **(M1)**–**(M3)** describe a large class of polygonal meshes that may include non-convex and degenerate (some of the angles are 180°) elements.

3.1 Discrete spaces

We now define the degrees of freedom for the discrete spaces X_h for velocities and Q_h for pressures. Let $\mathcal{E}_h^b$ indicate a subset of $\mathcal{E}_h$, defined later, and $\mathcal{E}_h^x$ indicate the set of remaining edges, $\mathcal{E}_h = \mathcal{E}_h^b \cup \mathcal{E}_h^x$.

For *velocities*, we take two degrees of freedom for each internal vertex of Ω_h, representing velocity at the point. In addition, and this is different with respect to the method of [4, 5], we add one degree of freedom for each edge $e \in \mathcal{E}_h^b$, representing a correction to the normal velocity on the edge. Every function $\mathbf{v}_h \in X_h$ is uniquely determined by the collection of real numbers

$$\{\mathbf{v}_h^\nu, v_h^e\}_{\nu\in\mathcal{N},\, e\in\mathcal{E}_h^b}.$$

Contrary to the finite element methods, we do not define explicitly the function $\mathbf{v}_h$ inside the mesh elements, but we require that

(A1) The tangential component of $\mathbf{v}_h$ on each edge $e \in \mathcal{E}_h$ is linear, and therefore uniquely determined by the value of $\mathbf{v}_h$ at two end-points of e.

(A2) On edge e of $\mathcal{E}_h^x$, the normal component is also linear, and the same observation as above holds.

(A3) On edge e of $\mathcal{E}_h^b$, the normal component of $\mathbf{v}_h$ is quadratic, and therefore uniquely determined by the values of $\mathbf{v}_h$ at the end-points ν and ν' of e and by identity

$$\int_e \mathbf{v}_h \cdot \mathbf{n}_e \,\mathrm{d}x = \frac{|e|}{2}(\mathbf{v}_h^\nu + \mathbf{v}_h^{\nu'}) \cdot \mathbf{n}_e + |e| v_h^e. \tag{3}$$

The identity (3) is what characterizes the underlying basis functions related to the edge degrees of freedom. Such functions play the same role as the edge bubbles in the standard finite element literature.

For *pressures*, we simply take one degree of freedom for each element E, representing the (constant) value of the pressure on the element. In the sequel, we indicate the real number $q_h|_E$ with q_E for all $E \in \Omega_h$. The discrete space of pressures is isomorphic to the space of piecewise constant functions on Ω_h, and this equivalence will be often implicitly used in the paper. Note that the space of discrete pressures must be corrected in order to be in $L_0^2(\Omega)$.

3.2 Discrete operators, bilinear forms and norms

We start introducing the mesh dependent H^1 local and global norms on X_h:

$$|||\mathbf{v}_h|||_E^2 = \sum_{e \in \partial E} h_e \|\frac{\partial \mathbf{v}_h}{\partial s}\|_{L^2(e)}^2 \qquad \forall \mathbf{v}_h \in X_h,\ \forall E \in \Omega_h\ , \tag{4}$$

where s represents the curvilinear abscissae along each edge. We then set

$$|||\mathbf{v}_h|||_{X_h}^2 = \sum_{E \in \Omega_h} |||\mathbf{v}_h|||_E^2\ . \tag{5}$$

In addition, we define the mesh dependent L^2-norm on Q_h:

$$\|q_h\|_{Q_h}^2 = \sum_{E \in \Omega_h} |E|\,(q_E)^2 \qquad \forall q_h \in Q_h$$

and the following seminorm:

$$|q_h|_h^2 = \sum_{e \in \mathcal{E}_h} h_e^2\, [\![q_h]\!]_e^2 \qquad \forall q_h \in Q_h,$$

where $[\![q_h]\!]_e$ denotes the jump of q_h across e.

The discrete divergence operator acting from X_h to Q_h is given by

$$\mathrm{div}_h(\mathbf{v}_h)|_E = \frac{1}{|E|} \sum_{e \in \partial E} \int_e \mathbf{v}_h \cdot \mathbf{n}_E^e \,\mathrm{d}x \qquad \forall \mathbf{v}_h \in X_h,\ E \in \Omega_h. \tag{6}$$

Note that both (4) and (6) are well defined since we know explicitly the functions of X_h on the boundary of each element.

Now, we introduce the bilinear form

$$\mathcal{A}_h : X_h \times X_h \longrightarrow \mathbb{R}$$

which mimics the continuous form $\mathcal{A}$ defined in (2), and is defined element-by-element:

$$\mathcal{A}_h(\mathbf{v}_h, \mathbf{w}_h) = \sum_{E \in \Omega_h} \mathcal{A}_E(\mathbf{v}_h|_E, \mathbf{w}_h|_E) \quad \forall \mathbf{v}_h, \mathbf{w}_h \in X_h.$$

Let $\overline{C}$ be the piecewise constant tensor given by the average of $C|_E$ on each element $E \in \Omega_h$. We then require the local bilinear forms $\mathcal{A}_E$ to satisfy the following *stability* and *consistency* conditions:

(S1) There exist two positive constants c_* and C_* independent of h such that, for all $E \in \Omega_h$ and $\mathbf{v}_E \in X_h|_E$, it holds

$$c_* |||\mathbf{v}_E|||_E^2 \leq \mathcal{A}_E(\mathbf{v}_E, \mathbf{v}_E) \leq C_* |||\mathbf{v}_E|||_E^2.$$

(S2) For all $E \in \Omega_h$, $\mathbf{v}_E \in X_h|_E$ and all linear vector functions $\mathbf{q}^1$ on E, it holds

$$\mathcal{A}_E(\mathbf{q}_I^1, \mathbf{v}_E) = \sum_{e \in \partial E} \int_e \left[(\overline{C} \nabla \mathbf{q}^1) \cdot \mathbf{n}_E^e\right] \cdot \mathbf{v}_E \, dx \ ,$$

where the interpolant $\mathbf{q}_I^1 \in X_h$ is defined by the collection of real numbers

$$\left\{(\mathbf{q}_I^1)^\nu = \mathbf{q}^1(\nu), \ q_I^e = 0\right\}_{\nu \in \mathcal{N}, e \in \mathcal{E}_h^b}$$

and assumptions **(A1)**–**(A3)**.

The condition **(S1)** represents the coercivity and correct scaling of the bilinear form. The condition **(S2)** mimicks an integration by parts. The algebraic construction of local bilinear forms which satisfy the above assumptions is shown in [4] for the case $\mathcal{E}_h^b = \mathcal{E}_h$. For the more general case considered here, this construction remains essentially identical; we simply erase the degrees of freedom associated with edges $e \in \mathcal{E}_h^x$. For completeness, we present briefly the main ideas behind the construction of the local stiffness matrices.

Let $\mathbf{A}_E$ be a $m_E \times m_E$ matrix associated with the bilinear form $\mathcal{A}_E$. Since $\mathbf{v}_E$ is arbitrary, the consistency condition **(S2)** may be written as six algebraic conditions

$$\mathbf{A}_E \, \mathbf{p}_i = \mathbf{s}_i, \qquad i = 1, \ldots, 6, \tag{7}$$

that correspond to six linear independent functions $\mathbf{q}^1$. We assume that the first two such functions are constant; therefore, $\mathbf{s}_1 = \mathbf{s}_2 = \mathbf{0}$.

We will apply a divide and conquer approach to find a matrix $\mathbf{A}_E$. Namely, we will provide a constructive way to build a special basis in $\mathbb{R}^{m_E}$, represented by columns of matrix $\mathbf{B}_E$, in which our matrix $\mathbf{A}_E$ is block-diagonal

$$\mathbf{B}_E^T \, \mathbf{A}_E \, \mathbf{B}_E = \begin{bmatrix} \widetilde{\mathbf{A}}_{E,1} & 0 \\ 0 & \widetilde{\mathbf{A}}_{E,2} \end{bmatrix}, \tag{8}$$

where the block $\widetilde{\mathbf{A}}_{E,1}$ is *computable* and the block $\widetilde{\mathbf{A}}_{E,2}$ can be *arbitrary* (for instance, the diagonal matrix $t\,\mathbf{I}$, where $t > 0$ is a free parameter) symmetric positive definite matrix. After that, the matrix $\mathbf{A}_E$ is calculated as a product of three matrices.

Lemma 3.1 *The columns of matrix* $\mathbf{B}_E$ *are as follows:*

$$\mathbf{b}_i = \mathbf{p}_i, \quad 1 \le i \le 6, \qquad \mathbf{b}_i^T \mathbf{b}_1^T = \mathbf{b}_i^T \mathbf{b}_2^T = \mathbf{b}_i^T \mathbf{s}_j = 0, \quad i \ge 7, \ j \ge 3.$$

The proof that vectors $\mathbf{b}_i$ form a basis in $\mathbb{R}^{m_E}$ can be found in [4]. The proof of orthogonality is short,

$$0 = \mathbf{b}_i^T \mathbf{s}_j = \mathbf{b}_i^T \mathbf{A}_E \, \mathbf{p}_j \equiv \mathbf{b}_i^T \mathbf{A}_E \, \mathbf{b}_j, \qquad j \le 6 < i.$$

Thus, the problem of building a special basis is reduced to a well know linear algebra problem of building a basis in a subspace of dimension $(m_E - 6)$. Calculation of entries of the matrix $\widetilde{\mathbf{A}}_{E,1}$ reduces to evaluation of bilinear form $\mathcal{A}_E$ for six linear independent basis functions $\mathbf{q}^1$. The consistency condition (**S2**) reduces this evaluation to edge integrals of linear functions.

3.3 The discrete problem, stability and convergence

We are now able to formulate our discrete method:

Find $\mathbf{u}_h \in X_h$ and $p_h \in Q_h$ such that

$$\begin{cases} \mathcal{A}_h(\mathbf{u}_h, \mathbf{v}_h) - \displaystyle\int_\Omega \mathrm{div}_h(\mathbf{v}_h)\, p_h \, \mathrm{d}x = \widehat{f}(\mathbf{v}_h) & \forall \mathbf{v}_h \in X_h, \\ \displaystyle\int_\Omega \mathrm{div}_h(\mathbf{u}_h)\, q_h \, \mathrm{d}x = 0 & \forall q_h \in Q_h \ , \end{cases} \tag{9}$$

where the loading term $\widehat{f}$ is obtained by approximating $\int_E f \, \mathrm{d}x$ with a element-wise integration rule based on the mesh nodes which is exact on constants.

Due to the coercivity condition (**S1**), the $h-$uniform stability of the above problem with respect to the discrete norms $|||\cdot|||_{X_h}$ and $||\cdot||_{Q_h}$ is guaranteed provided that (see for example [12]) the following inf-sup condition holds.

Condition 3.1 *It exists a positive real constant β, independent of h, such that*

$$\sup_{\mathbf{v}_h \in X_h/\{\mathbf{0}\}} \frac{\displaystyle\int_\Omega \mathrm{div}_h(\mathbf{v}_h)\, q_h \, \mathrm{d}x}{|||\mathbf{v}_h|||_{X_h}} \ge \beta ||q_h||_{Q_h} \qquad \forall q_h \in Q_h. \tag{10}$$

Under this condition, the linear convergence of the method in the above discrete norms is proved in [5], provided that the solution $(\mathbf{u}, p)$ is in $(H^2(\Omega))^2 \times H^1(\Omega)$, and the tensor $C|_E \in W^{1,\infty}(E)$ for all $E \in \Omega_h$. Conversely, the failure of (10) implies the presence of discrete spurious pressure modes and in general a bad behavior of the method; therefore, Condition 3.1 is crucial.

In [5], such condition is shown to hold for the case $\mathcal{E}_h^b = \mathcal{E}_h$. The role of the edge-based degrees of freedom is only to guarantee (10). In this paper, we show that setting $\mathcal{E}_h^b = \mathcal{E}_h$ means adding far too much useless degrees of freedom to the system. In other words, we will show how a smaller set of edges $\mathcal{E}_h^b$ is often sufficient to guarantee Condition 3.1.

4 A general macroelement technique

In this section, we extend the finite element results of [30] proved for simplicial meshes to the case of mimetic finite differences on polygonal meshes satisfying **(M1)**–**(M3)**. The main result of this section, Theorem 4.1, will follow from a set of four Lemmas. We will skip all the proofs which are essentially identical to the original ones of [30].

4.1 Elements and macroelements

Let us introduce the concept of macroelement and equivalence class of macroelements. We observe that, due to conditions **(M1)**–**(M3)**, for each integer number $3 \leq n \leq \bar{N}$ there exists a reference element $\widehat{E}_n$ such that the following holds. Every element E in Ω_h with n edges is the image of an invertible and continuous map

$$F_E : \widehat{E}_n \longrightarrow E \ . \tag{11}$$

Moreover, the map F_E and its inverse are piecewise $W^{1,\infty}$ with respect to the auxiliary triangulation of $\widehat{E}_n$ into n triangles defined in **(M3)**.

The result above is easy to prove in the following way. Let us define $\widehat{E}_n$ as a convex regular polygon with n edges and build a triangulation of $\widehat{E}_n$ connecting all its vertexes with the baricenter $\widehat{x}$. Then, for each element $E \in \Omega_h$. the mapping F_E is the only piecewise linear function $\widehat{E}_n \to E$ which sends ordered vertexes of $\widehat{E}_n$ in ordered vertexes of E and $\widehat{x}$ in the point x_E defined in **(M2)**. Due the shape-regularity assumption **(M3)**, the $W^{1,\infty}$ regularity of F_E can be shown with standard arguments from the FE literature.

A *macroelement* M is a connected collection of elements. Given a mesh Ω_h, we indicate with $\mathcal{M}_h$ a collection of macro-elements which covers the whole mesh, i.e. for all $E \in \Omega_h$ it holds $E \in M$ for some macroelement $M \in \mathcal{M}_h$.

Given $M \in \mathcal{M}_h$, we introduce local spaces:

$$\begin{aligned} X_M^0 &= \{\mathbf{v}_h \in X_h|_M \ : \ \mathbf{v}_h^\nu = \mathbf{0} \quad \forall \nu \in \mathcal{N} \cap \partial M, \quad v_h^e = 0 \quad \forall e \in \mathcal{E}_h^b \cap \partial M\}, \\ Q_M &= Q_h|_M \ . \end{aligned} \tag{12}$$

We introduce also the following norm and seminorm:

$$\begin{aligned} |||\mathbf{v}_M|||_M^2 &= \sum_{E \in M} |||\mathbf{v}_M|||_E^2 \qquad \forall \mathbf{v}_M \in X_M^0 \ , \\ |q_M|_M^2 &= \sum_{e \in \mathcal{E}_h^M} h_e^2 \, [\![q_M]\!]_e^2 \qquad \forall q_M \in Q_M \ , \end{aligned} \tag{13}$$

where $\mathcal{E}_h^M$ represents the internal edges of M.

Finally, we introduce the equivalence class of macroelements.

Definition 4.1 *A macroelement is said to be equivalent with a reference macroelement $\widehat{M}$ if there exists an invertible continuous mapping $F_M : \widehat{M} \to M$ such that:*

- $F_M(\widehat{M}) = M$,
- *If $\widehat{M} = \cup_{j=1}^m \widehat{E^j}$ and $M = \cup_{j=1}^m E^j$, then $E^j = F_M(\widehat{E^j})$. Moreover both E^j and $\widehat{E^j}$ have the same number of edges, n_j.*

- $F_M|_{\widehat{E^j}} = F_{E^j} \circ F_{\widehat{E^j}}^{-1}$, $j = 1, 2, ..., m$, *where* F_{E^j} *and* $F_{\widehat{E^j}}$ *are the mappings from the reference element* $\widehat{E}_{n_j}$, *introduced in* (11), *into* E^j *and* $\widehat{E^j}$, *respectively.*

Two macroelements which are equivalent to the same reference macroelement are said to be equivalent.

4.2 A stability result using macroelements

The proof of the following lemma is essentially identical to that in Lemma 1 of [30] and therefore not shown.

Lemma 4.1 *Assume that there exists a macroelement partition* $\mathcal{M}_h$ *such that each* $e \in \mathcal{E}_h$ *is an interior edge of at least one and not more than* $\bar{L}$ *macroelements, where* $\bar{L}$ *is independent of* h. *Moreover, assume that there exists a positive constant* β_1 *such that*

$$\sup_{\mathbf{v}_M \in X_M^0/\{\mathbf{0}\}} \frac{\displaystyle\int_\Omega \mathrm{div}_h(\mathbf{v}_M)\, q_M \,\mathrm{d}x}{|||\mathbf{v}_M|||_M} \geq \beta_1 |q_M|_M \qquad \forall q_M \in Q_M. \tag{14}$$

Then, there exist a positive constant β_2 *such that*

$$\sup_{\mathbf{v}_h \in X_h/\{\mathbf{0}\}} \frac{\displaystyle\int_\Omega \mathrm{div}_h(\mathbf{v}_h)\, q_h \,\mathrm{d}x}{|||\mathbf{v}_h|||_{X_h}} \geq \beta_2 ||q_h||_h \qquad \forall q_h \in Q_h\ . \tag{15}$$

Lemma 4.2 *There exist two positive constants* β_1 *and* β_2, *independent of* h, *such that*

$$\sup_{\mathbf{v}_h \in X_h/\{\mathbf{0}\}} \frac{\displaystyle\int_\Omega \mathrm{div}_h(\mathbf{v}_h)\, q_h \,\mathrm{d}x}{|||\mathbf{v}_h|||_{X_h}} \geq \beta_1 ||q_h||_{Q_h} - \beta_2 ||q_h||_h \qquad \forall q_h \in Q_h\ . \tag{16}$$

Proof. The proof is an extension of that in Lemma 2 of [30]. Due to the well known inf-sup condition [12] for the continuous problem, for any $p \in L_0^2(\Omega)$ there exists $\mathbf{v} \in (H^1(\Omega))^2$ and a positive constant C_1 independent of h, such that

$$\int_\Omega \mathrm{div}(\mathbf{v})\, q_h \,\mathrm{d}x \geq C_1 ||q_h||_{Q_h} \qquad \text{and} \qquad ||\mathbf{v}||_{(H^1(\Omega))^2} = 1. \tag{17}$$

Let $\mathbf{v}^c$ be the Clément interpolant of $\mathbf{v}$ on the auxiliary triangular mesh in Ω_h introduced in **(M3)**, and $\mathbf{v}_h$ be the element in X_h defined uniquely by the collection

$$\{\mathbf{v}_h^\nu = \mathbf{v}^c(\nu),\ \mathbf{v}_h^e = 0\}_{\nu \in \mathcal{N}, e \in \mathcal{E}_h^b}.$$

Then, there exists a positive constant C_2 such that

$$\left(\sum_{E \in \Omega_h} h_E^{-2} ||\mathbf{v} - \mathbf{v}^c||_{(L^2(E))^2}^2 + \sum_{e \in \mathcal{E}_h} h_e^{-1} ||\mathbf{v} - \mathbf{v}^c||_{(L^2(e))^2}^2 \right)^{1/2} \leq C_2 ||\nabla \mathbf{v}||_{(L^2(\Omega))^{2\times 2}}. \tag{18}$$

First the definition of norm on X_h and a scaling argument using the regularity of the auxiliary triangular mesh, then a standard result for the Clément interpolant, yield the existence of two positive constants C_3' and C_3 independent of h such that

$$|||\mathbf{v}_h|||_{X_h} \leq C_3' ||\nabla \mathbf{v}^c||_{(L^2(\Omega))^{2\times 2}} \leq C_3 ||\mathbf{v}||_{(H^1(\Omega))^2} = C_3. \tag{19}$$

Due to **(A1)**–**(A3)** and since $\mathbf{v}^c$ is linear on each edge, it holds $\mathbf{v}_h|_e = \mathbf{v}^c|_e$ for all edges e in the mesh. Therefore, recalling that q_h is a piecewise constant function and using the integration by parts, we get

$$\int_E \mathrm{div}_h(\mathbf{v}_h)\, q_h \,\mathrm{d}x = q_E \sum_{e\in\partial E} \int_e \mathbf{v}_h \cdot \mathbf{n}_E^e \,\mathrm{d}x = q_E \sum_{e\in\partial E} \int_e \mathbf{v}^c \cdot \mathbf{n}_E^e \,\mathrm{d}x = \int_E \mathrm{div}(\mathbf{v}^c)\, q_h \,\mathrm{d}x \tag{20}$$

for all E in Ω_h.

Using (20), the first inequality in (17), an elementwise integration by parts, and finally bound (18) together with the second inequality of (17), we obtain

$$\begin{aligned}
\int_\Omega \mathrm{div}_h(\mathbf{v}_h)\, q_h \,\mathrm{d}x &= \int_\Omega \mathrm{div}(\mathbf{v})\, q_h \,\mathrm{d}x + \int_\Omega \mathrm{div}(\mathbf{v}^c - \mathbf{v})\, q_h \,\mathrm{d}x \\
&\geq C_1 ||q_h||_{Q_h} + \sum_{e\in\mathcal{E}_h} [\![q_h]\!]_e \int_e (\mathbf{v}^c - \mathbf{v}) \cdot \mathbf{n}_e \,\mathrm{d}x \\
&\geq C_1 ||q_h||_{Q_h} - ||q_h||_h \left(\sum_{e\in\mathcal{E}_h} h_e^{-1} \int_e |\mathbf{v}^c - \mathbf{v}|^2 \,\mathrm{d}x \right)^{1/2} \\
&\geq C_1 ||q_h||_{Q_h} - C_2 ||q_h||_h .
\end{aligned} \tag{21}$$

The assertion of the lemma follows immediately combining (21) with (19) and setting $\beta_1 = C_1 C_3^{-1}$ and $\beta_2 = C_2 C_3^{-1}$. □

The following result follows easily using Lemma 4.2, see Lemma 3 of [30] for details of the proof.

Lemma 4.3 *Let the stability estimate* (15) *hold. Then Condition 3.1 is valid.*

The following fundamental result also holds.

Lemma 4.4 *Let Σ be a class of equivalent macroelements. Suppose that for every $M \in \Sigma$ the space*

$$\mathcal{N}_M = \{ q_M \in Q_M \ : \ \int_M \mathrm{div}_h(\mathbf{v}_M)\, q_M \,\mathrm{d}x = 0 \quad \forall \mathbf{v}_M \in X_M^0 \} \tag{22}$$

is one dimensional consisting of functions which are constant on M. Then, there exists a constant β', independent of h, such that

$$\sup_{\mathbf{v}_M \in X_M^0/\{0\}} \frac{\int_\Omega \mathrm{div}_h(\mathbf{v}_M)\, q_M dx}{|||\mathbf{v}_M|||_M} \geq \beta' |q_M|_M \qquad \forall q_M \in Q_M \tag{23}$$

holds for all $M \in \Sigma$.

Proof. The proof is an extension of that in Lemma 4 of [30]. For a particular macroelement M, we shall write β'_M to stress the fact that this constant depends on M. Since $\mathcal{N}_M$ consists of only constant functions, $\beta'_M > 0$. With a proper coordinate transformation, it is sufficient to consider a class of equivalent macroelements of diameter ≤ 1. Definition 4.1 of macroelement classes implies that every $M \in \Sigma$ and the related reference mappings are defined uniquely by the position of a finite number of vertices $\{x^1, ..., x^m\}$ and the position of the internal points x_E, $E \in M$, defined in **(M2)**. Let $X = X(M)$ represent the vector in $\mathbb{R}^{2m+2\overline{m}}$ with components given by the ordered components of $\{x^1, ..., x^m, x_{E_1}, ..., x_{E_{\overline{m}}}\}$. Let Σ_X indicate the set of all admissible vectors X which are associated to all admissible macroelements $M = M(X) \in \Sigma$. Clearly Σ_X is a bounded subset of $\mathbb{R}^{2m+2\overline{m}}$ due to the above diameter property. It can be checked that, due to property **(M3)**, the set Σ_X is also closed. In fact, such property forbids the vectors in Σ_X to be arbitrarily close to unadmissible vectors $\bar{X} \notin \Sigma_X$, like those where two vertexes are collapsed into a single vertex.

Thus, the equivalence class Σ_X forms a compact set. Therefore, if we indicate with $\beta'(X)$ the inf-sup constant associated to the macroelement M defined by X, i.e. $\beta'(X) = \beta'_{M(X)}$, all we need to show is that the function $\beta'(X)$ is continuous.

This is done by a simple change of variables argument, which is presented briefly. Given any two macroelements $M = M(X)$ and $M' = M'(X')$, we introduce the invertible mapping $G = F_{M'} \circ F_M^{-1}$, where F_M and $F_{M'}$ are the mappings introduced in Definition 4.1. Using this mapping, we can transform all variables and integrals appearing in (23) from M to M'. The Jacobian of G appears in all these transformations. It is easy to check that the Jacobian converges uniformly to the identity when $X \to X'$. Thus, the terms

$$\int_\Omega \mathrm{div}_h(\mathbf{v}_M)\, q_M \,\mathrm{d}x, \qquad |||\mathbf{v}_M|||_M, \qquad |q_M|_M$$

converge to their counterparts in M' when $X \to X'$. This clearly implies that $\beta(X) \to \beta(X')$ when $X \to X'$. □

Combining Lemmata 4.1, 4.3 and 4.4, we get the main result of this section.

Theorem 4.1 *Let $\mathcal{M}_h$ be a macroelement partition of Ω_h. Suppose that*

1. *$\mathcal{M}_h$ is composed of a fixed set of equivalence classes Σ_i, $i = 1, 2, \ldots, l$, of macroelements, i.e. $\mathcal{M}_h = \cup_{i=1}^l \Sigma_i$.*

2. *For each $M \in \Sigma_i$, $i = 1, 2, ..., l$, the space $\mathcal{N}_M$ in (22) is one-dimensional consisting of functions that are constant on M.*

3. *There exists $\bar{L} \in \mathbb{N}$ such that each $e \in \mathcal{E}_h$ is an interior edge of at least one and no more than $\bar{L}$ macroelements.*

Then Condition 3.1 holds.

5 A stability result for the MFD method

Given any polygonal mesh Ω_h satisfying **(M1)**–**(M3)**, we introduce a macroelement partition $\mathcal{M}_h$ which verifies the hypotheses of Theorem 4.1. The results in this section provide flexible tools for identifying the stabilizing set $\mathcal{E}_h^b$ of edge bubbles.

We start introducing the macroelement family. Given any internal node $\nu \in \mathcal{N}$ which is common for at least three edges, we indicate with $M = M_\nu$ the macroelement given by all elements in Ω_h which have ν as a vertex. Note that all such macroelements clearly cover (with overlaps) the whole mesh Ω_h (see Fig. 1).

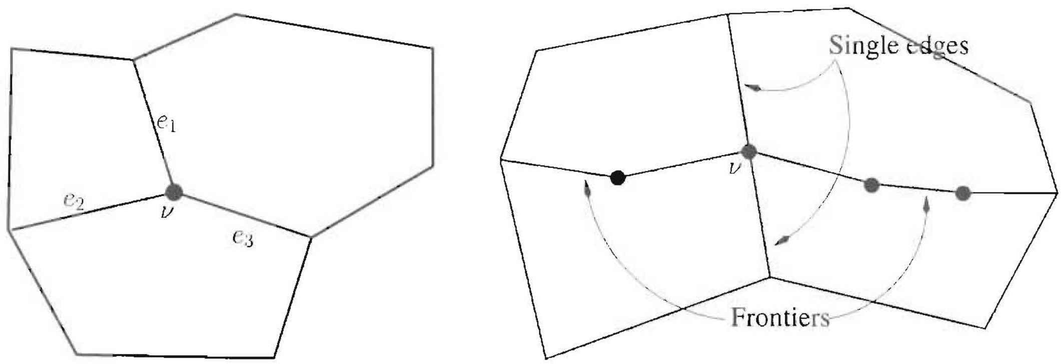

Figure 1: Examples of macroelements.

For each internal edge of the mesh $e \in \mathcal{E}_h$ there exists at least one macroelement with e as an internal edge. Moreover, it is easy to check that any edge $e \in \mathcal{E}_h$ lays at most in 2 macroelements, and therefore condition 3 in Theorem 4.1 is verified.

In order to verify condition 1 in Theorem 4.1, we need to count the number of equivalence classes Σ_i in $\mathcal{M}_h$. Two macroelements M_ν and $M_{\nu'}$ are surely equivalent if

1. The number of polygons in M_ν is equal to the number of polygons in $M_{\nu'}$. We refer this number as $k(\nu)$.

2. The number of edges in polygons $E_1, E_2, ..., E_{k(\nu)}$, ordered counter-clockwise about vertex ν, is the same as that in polygons $E'_1, E'_2, ..., E'_{k(\nu)}$, ordered counter-clockwise about vertex ν'.

3. The number of edges in $\partial E_i \cap \partial E_{i+1}$ are equal to the number of edges in $\partial E'_i \cap \partial E'_{i+1}$ for $i = 1, 2, ..., k(\nu)$ (modulo $k(\nu)$).

For any vertex ν, the shape regularity assumption **(M3)** implies that $k(\nu) \leq \bar{K}$ with $\bar{K}$ independent of h. Moreover, due to **(M1)**, each polygon has at most $\bar{N}$ edges; hence, any set $\partial E_i \cap \partial E_j$ has at most $\bar{N} - 1$ edges. Therefore, since there exist at most $l = l(\bar{K}, \bar{N})$ equivalence classes in $\mathcal{M}_h$, condition 1 is satisfied.

It remains to show condition 2, which is more involved. Given an internal node ν and the respective macroelement M_ν, let $\mathcal{E}_\nu$ be the set of mesh edges which join at ν. We also introduce subsets $\mathcal{E}_\nu^x = \mathcal{E}_\nu \cap \mathcal{E}_h^x$ and $\mathcal{E}_\nu^b = \mathcal{E}_\nu \cap \mathcal{E}_h^b$. Let N_ν, N_ν^x, and N_ν^b be the number of elements in the sets $\mathcal{E}_\nu$, $\mathcal{E}_\nu^x$, and $\mathcal{E}_\nu^b$, respectively.

Proposition 5.1 *Let ν be the only internal vertex in M_ν. Furthermore, let either (a) $N_\nu^x < 3$ or (b) $N_\nu^x = 3$ and all the three angles naturally defined by the three edges in $\mathcal{E}_\nu \cap \mathcal{E}_h^x$ be less or equal than π. Then, the space $\mathcal{N}_M$ defined in* (22) *consists of constant functions.*

Proof. We divide the proof into three steps.

Step 1. We start with case $N_\nu^x = 3$ (see left picture in Fig. 1). For each edge e in $\mathcal{E}_\nu$, let $\boldsymbol{\tau}_e$ indicate the unit edge tangent, pointing outwards with respect to ν. Moreover, let the edge normal $\mathbf{n}_e$ be such that

$$\boldsymbol{\tau}_e = (\tau_e^x, \tau_e^y) = (-n_e^y, n_e^x),$$

i.e. $\boldsymbol{\tau}_e$ is obtained with the counter-clockwise rotation of $\mathbf{n}_e$ by angle $\pi/2$. Given any edge $e \in \partial E \cap \partial E'$ with $\mathbf{n}_e$ the outward normal for E, we define the jump of q_h across e as

$$[\![q_h]\!]_e = q_E - q_{E'}.$$

Finally, we enumerate the three edges in $\mathcal{E}_\nu^x$ as e_1, e_2, e_3, their tangents as $\boldsymbol{\tau}_1, \boldsymbol{\tau}_2, \boldsymbol{\tau}_3$ and their normals as $\mathbf{n}_1, \mathbf{n}_2, \mathbf{n}_3$. Without loss of generality, we assume that $\boldsymbol{\tau}_1$ and $\boldsymbol{\tau}_2$ are linearly independent. The remaining edges in $\mathcal{E}_\nu$ are then enumerated as $e_4, e_5, ...$, with the respective enumeration of their tangents and normals.

Let $q_h \in \mathcal{N}_M$. Since $\mathbf{v}_h$ is zero on the boundaries of M, the straightforward calculation gives

$$0 = \int_M \operatorname{div}_h(\mathbf{v}_h)\, q_h \,\mathrm{d}x = \sum_{E\in M}\sum_{e\in\partial E} q_E \int_e \mathbf{v}_h\cdot\mathbf{n}_E \,\mathrm{d}x = \sum_{e\in\mathcal{E}_\nu} [\![q_h]\!]_e \int_e \mathbf{v}_h\cdot\mathbf{n}_e\,\mathrm{d}x \qquad \forall \mathbf{v}_h \in X_M^0. \tag{24}$$

Let $\mathbf{w} = \mathbf{v}_h^\nu$ for simplicity. Recalling identity (3), equation (24) becomes

$$0 = \frac{1}{2}\sum_{e\in\mathcal{E}_\nu} |e|\, [\![q_h]\!]_e\, \mathbf{w}\cdot\mathbf{n}_e + \sum_{e\in\mathcal{E}_\nu^b} |e|\, [\![q_h]\!]_e\, v_b^e \qquad \forall \mathbf{v}_h \in X_M^0. \tag{25}$$

By definition of jump, we clearly get

$$\sum_{e\in\mathcal{E}_\nu} [\![q_h]\!]_e = 0\ . \tag{26}$$

Proving the proposition is therefore equivalent to showing that, under conditions (26) and (25), all the jumps $[\![q_h]\!]_e$, $e \in \mathcal{E}_\nu$, are zero.

Step 2. Taking $\mathbf{w} = 0$ and $v_h^e = 1$ for a particular edge in $\mathcal{E}_\nu^b$ and $v_h^e = 0$ for the remaining edges, we conclude that $[\![q_h]\!]_e$ for all edges in $\mathcal{E}_\nu^b$.

Let $\mathbf{w}_1, \mathbf{w}_2$ be a basis in $\mathbb{R}^2$. Writing condition (25) separately for $\mathbf{w}_1$ and $\mathbf{w}_2$ and adding condition (26), we obtain a linear system of equations

$$\mathbf{S}\,\mathbf{q} = \mathbf{0}, \tag{27}$$

where the vector $\mathbf{q}$ has three components, $\mathbf{q} = ([\![q_h]\!]_{e_1}, [\![q_h]\!]_{e_2}, [\![q_h]\!]_{e_3})$, and the square matrix $\mathbf{S}$ has the form

$$\mathbf{S} = \begin{pmatrix} |e_1|\mathbf{w}_1\cdot\mathbf{n}_1 & |e_2|\mathbf{w}_1\cdot\mathbf{n}_2 & |e_3|\mathbf{w}_1\cdot\mathbf{n}_3 \\ |e_1|\mathbf{w}_2\cdot\mathbf{n}_1 & |e_2|\mathbf{w}_2\cdot\mathbf{n}_2 & |e_3|\mathbf{w}_2\cdot\mathbf{n}_3 \\ 1 & 1 & 1 \end{pmatrix}. \tag{28}$$

Our goal is to show that the matrix $\mathbf{S}$ has full rank. Recalling that $\boldsymbol{\tau}_1$ and $\boldsymbol{\tau}_2$ are linearly independent by hypothesis, we have

$$\boldsymbol{\tau}_1\cdot\mathbf{n}_1 = \boldsymbol{\tau}_2\cdot\mathbf{n}_2 = 0\ , \qquad \boldsymbol{\tau}_1\cdot\mathbf{n}_2 = -\boldsymbol{\tau}_2\cdot\mathbf{n}_1 \neq 0\ . \tag{29}$$

Taking the choice $\mathbf{w}_1 = \boldsymbol{\tau}_1$ and $\mathbf{w}_2 = \boldsymbol{\tau}_2$, calculating the determinant in (28) and using (29) one easily gets the equivalent condition

$$|e_3|\mathbf{n}_3 \cdot (|e_2|\boldsymbol{\tau}_2 - |e_1|\boldsymbol{\tau}_1) \neq |e_1||e_2|(\boldsymbol{\tau}_2 \cdot \mathbf{n}_1) . \tag{30}$$

By the angle hypothesis of the Proposition, it is easy to check that there must exist two real numbers α_1, α_2 such that

$$\boldsymbol{\tau}_3 = -\alpha_1\boldsymbol{\tau}_1 - \alpha_2\boldsymbol{\tau}_2 , \qquad \alpha_1 \geq 0, \ \alpha_2 \geq 0 . \tag{31}$$

From (31) it immediately follows that $\mathbf{n}_3 = -\alpha_1\mathbf{n}_1 - \alpha_2\mathbf{n}_2$. Substitutinf this into (30) and using (29) we show that condition (30) is equivalent to

$$|e_3|(-\alpha_1|e_2| - \alpha_2|e_1|)\boldsymbol{\tau}_2 \cdot \mathbf{n}_1 \neq |e_1||e_2|\boldsymbol{\tau}_2 \cdot \mathbf{n}_1 . \tag{32}$$

Since both α_1 and α_2 are non-negative, the equality in (32) is surely impossible. Therefore, the matrix $\mathbf{S}$ in (28) is non-singular and the proposition is proved for $N_\nu^x = 3$.

Step 3. In the case $N_\nu^x = 2$, we can follow the same argument and calculations as above. We end up with showing that the matrix

$$\mathbf{S} = \begin{pmatrix} |e_1|\mathbf{w}_1 \cdot \mathbf{n}_1 & |e_2|\mathbf{w}_1 \cdot \mathbf{n}_2 \\ |e_1|\mathbf{w}_2 \cdot \mathbf{n}_1 & |e_2|\mathbf{w}_2 \cdot \mathbf{n}_2 \\ 1 & 1 \end{pmatrix} \tag{33}$$

has full rank. Clearly, it could be rank deficient only when $\mathbf{n}_1 = \mathbf{n}_2$, which is impossible. The cases $N_\nu^x = 0$ and $N_\nu^x = 1$ are even simpler and therefore not shown. □

Note that the angle condition in Proposition 5.1 is sharp in the following sense. It can be shown that, if $N_\nu^x = 3$, then for any triple $\boldsymbol{\tau}_1, \boldsymbol{\tau}_2, \boldsymbol{\tau}_3$ that does not satisfy the angle condition there exists at least one triple of edges e_1, e_2, e_3 (with the $\boldsymbol{\tau}_i$ as respective tangents) such that the matrix in (28) is singular.

A stronger result follows easily from Proposition 5.1. In the sequel we call a *frontier* $\widetilde{e}$ any collection of *at least two* adjoint edges such that $\widetilde{e} = \partial E \cap \partial E'$, with $E, E' \in M_\nu$ (see right picture in Fig. 1). By our assumptions, Proposition 5.1 considers only macroelements with no frontiers. In a general case, all the internal boundaries among elements in M can be divided into frontiers and regular (single) edges. The next result shows that frontiers can be essentially ignored.

Proposition 5.2 *Let $\bar{N}_\nu^x$ indicate the number of edges of $\mathcal{E}_h^x$ which connect in ν and which are not a part of a frontier. Let either (a) $\bar{N}_\nu^x < 3$ or (b) $\bar{N}_\nu^x = 3$ and all the three angles naturally defined by the three respective edges be less or equal than π. Then, the space $\mathcal{N}_M$ defined in* (22) *consists of constant functions.*

Proof. Let $\widetilde{e}$ be a frontier in M, with $\widetilde{e} = \partial E \cap \partial E'$, $E, E' \in M$. Let $\nu' \neq \nu$ be one of the interior vertices in $\widetilde{e}$ and let e', e'' be the two edges in $\widetilde{e}$ adjacent to ν'. Let $\mathbf{v}_h$ be zero in all interior vertices except ν', and $v_h^e = 0$ for all edges in $\mathcal{E}_\nu^b$. We define $\mathbf{w} = \mathbf{v}_h^{\nu'}$ for simplicity. Testing condition (22) with such $\mathbf{v}_h$, we easily obtain

$$\begin{aligned} 0 = \int_M \mathrm{div}_h(\mathbf{v}_h)\, q_h \,\mathrm{d}x &= [\![q_h]\!]_{\widetilde{e}} \left(\int_{e'} \mathbf{v}_h \cdot \mathbf{n}_E^{e'} \,\mathrm{d}x + \int_{e''} \mathbf{v}_h \cdot \mathbf{n}_E^{e''} \,\mathrm{d}x \right) \\ &= [\![q_h]\!]_{\widetilde{e}} \, \frac{1}{2}\left(|e'|\mathbf{w} \cdot \mathbf{n}_E^{e'} + |e''|\mathbf{w} \cdot \mathbf{n}_E^{e''} \right) \qquad \forall \mathbf{w} \in \mathbb{R}^2 , \end{aligned} \tag{34}$$

where $[\![q_h]\!]_{\tilde{e}} = q_E - q_{E'}$ represents the jump across the frontier. It is easy to check that condition (34) implies $[\![q_h]\!]_{\tilde{e}} = 0$, i.e. that $q_E = q_{E'}$. As a consequence, the two elements E and E' can be considered as a single element for the purposes of this proof, and the frontier $\tilde{e}$ can be completely ignored. Note also that this argument does not use the degrees of freedom related to the node ν, nor any degree of freedom related to an edge bubble. Since this argument can be applied to all frontiers in M, they all can be ignored by considering the respective pairs of elements as single elements. The remaining proof of this proposition boils down to that of Proposition 5.1. □

We have shown that, provided the set $\mathcal{E}_h^b$ is such that the conditions in Proposition 5.2 are satisfied, condition 3 in Theorem 4.1 is also verified. This in turn implies the stability and (linear) convergence of the method, as discussed in Section 3.3.

The above result covers, for example, the case of a mesh with convex elements where all the nodes have the property of being the junction of at most 3 edges. For example, the Voronoi meshes satisfy this property and in such a case the result shows that no bubble degrees of freedom are needed, i.e. $\mathcal{E}_h^b = \emptyset$ is sufficient. For a logically square mesh, we need to add bubble degrees of freedom approximately to every fourth edge. This is sufficient to kill spurious pressure modes.

In a more general case, it is sufficient to add bubbles where needed, as indicated in Proposition 5.2. A few bubble degrees of freedom are therefore often sufficient for the stability of the method; it is quite clear that in general taking $\mathcal{E}_h^b = \mathcal{E}_h$ as proposed in [4] is not the optimal choice.

6 Numerical experiments

As it was shown in [28] the LBB constant β is related to the smallest eigenvalues of a generalized eigenvalue problem. In our experiments, we use the power method to calculate this eigenvalue. To identify edges where the stabilizing bubbles have to be added, we employ the following simple algorithm. For each mesh vertex, we count the number of connected edges excluding frontiers. If the final count is greater than three, we add a bubble degree of freedom to one (or more) the edges in the list. The following relative errors are calculated in numerical experiments:

$$\varepsilon_1(\mathbf{u}) = \frac{|||\mathbf{u}_h - \mathbf{u}_I|||_{X_h}}{|||\mathbf{u}_I|||_{X_h}}, \qquad \varepsilon_0(p) = \frac{||p_h - p_I||_{Q_h}}{||p_I||_{Q_h}},$$

and

$$\varepsilon_0(\mathbf{u}) = \frac{|||\mathbf{u}^h - \mathbf{u}_I|||_0}{|||\mathbf{u}_I|||_0}, \qquad |||\mathbf{u}_h|||_0 = \left(\sum_E |E| \sum_{\nu\in E} |\mathbf{u}_h^\nu|^2\right)^{1/2},$$

where $p_I \in Q_h$ is the interpolant of p and $\mathbf{u}_I \in X_h$ is the interpolant of $\mathbf{u}$.

In the first experiment, we consider a sequence of convex polygonal meshes that are dual to unstructured quasi-uniform Delaunay meshes (see Fig. 2). Each mesh vertex is common to at most three edges. Therefore, no stabilizing bubbles are required and the discrete problem with purely nodal velocity space is fully stable. This is a nice property which is not shared by standard FEM meshes, apart for particular configurations.

Let the exact solution be

$$\mathbf{u}(x,\,y) = \begin{pmatrix} r(x)\sin(a\,y) \\ r'(x)\cos(a\,y)/a \end{pmatrix}, \qquad p(x,\,y) = xy^2, \tag{35}$$

where $r(x) = (1-x)\sin(a\,x)$, r' is its first derivative, and $a = 2.2\,\pi$. Table 1 shows that β is independent of the characteristic mesh size h. We observe the second-order convergence rate for the velocity in the discrete L^2-norm and the first-order in the discrete H^1-norm. The convergence rate for the pressure variable approaches the first-order. This is in agreement with our theoretical analysis.

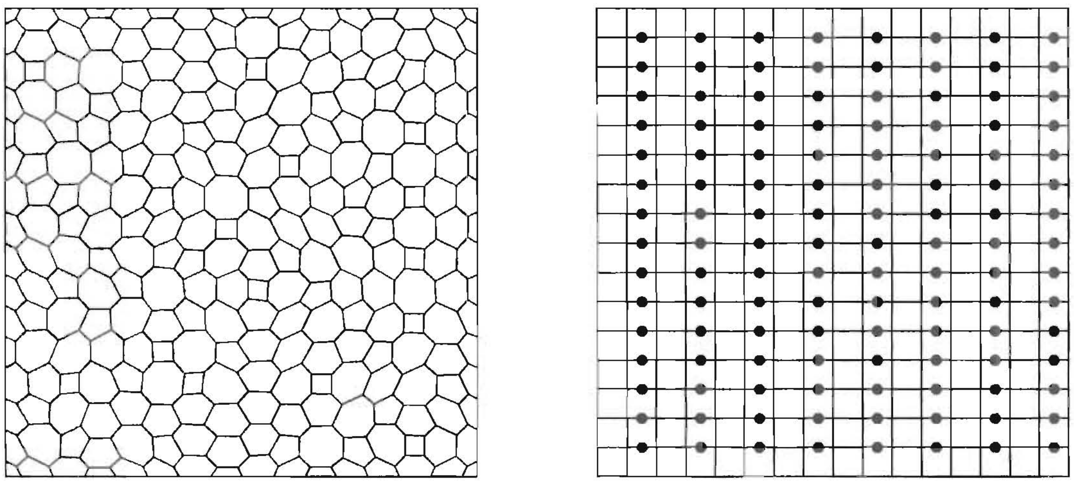

Figure 2: A unstructured polygonal mesh (left) and location of bubbles on the square mesh (right).

$1/h$	β	$\varepsilon_0(\mathbf{u})$	$\varepsilon_1(\mathbf{u})$	$\varepsilon_0(p)$
8	4.25e-2	1.24e-1	1.71e-1	1.97e-0
16	3.72e-2	3.21e-2	6.83e-2	5.42e-1
32	3.48e-2	7.74e-3	2.73e-2	1.79e-1
64	3.38e-2	1.92e-3	1.26e-2	6.79e-2
128	3.35e-2	4.77e-4	6.13e-3	2.91e-2

Table 1: MFD discretization without bubble degrees of freedom on polygonal meshes.

In the second experiment, we consider a sequence of square meshes and the exact solution (35). Table 2 shows results for the case when no bubble degrees of freedom is added to the MFD discretizations. It is known that $\beta = 0$ in this case due to a spurious pressure mode. This mode is known for the square mesh and has a chess-board pattern, with $+1$ and -1 corresponding to white and black cells, respectively. Therefore, we present the smallest non-zero eigenvalue that can be interpreted as the LBB constant $\beta^\perp$ for the pressure space orthogonal to the null mode. The calculations are performed in the corrected pressure space, orthogonal to the null mode. Note that $\beta^\perp$ is scaled as $O(h^2)$ which may result in potential instabilities in simulations. These instabilities are not observed in our experiments which allows us to compare the calculated errors with the MFD method with stabilized bubble degrees of freedom (see Table 3).

$1/h$	$\beta^{\perp}$	$\varepsilon_0(\mathbf{u})$	$\varepsilon_1(\mathbf{u})$	$\varepsilon_0(p)$
8	1.78e-2	1.62e-1	1.23e-1	3.52e-0
16	4.65e-3	4.64e-2	3.88e-2	8.49e-1
32	1.18e-3	1.20e-2	1.04e-2	2.10e-1
64	2.99e-4	3.04e-3	2.64e-3	5.23e-2
128	7.50e-5	7.62e-4	6.63e-4	1.31e-2

Table 2: MDF discretization without bubble degrees of freedom on square meshes.

Figure 2 shows location of edges where additional degrees of freedom are added, roughly a quarter of all edges. In this case, as indicated by the values of $beta$, the discrete problem is uniformly stable and we do not need to orthogonalize the pressure space. In both cases, the superconvergence is observed for the H^1-norm of the velocity error. However, the actual convergence rate is slightly smaller in the stabilized experiments. Similar behavior is observed for pressure errors.

$1/h$	β	$\varepsilon_0(\mathbf{u})$	$\varepsilon_1(\mathbf{u})$	$\varepsilon_0(p)$
8	1.29e-1	1.57e-1	1.24e-1	3.55e-0
16	1.30e-1	4.35e-2	4.41e-2	1.20e-0
32	1.29e-1	1.13e-2	1.46e-2	4.25e-1
64	1.32c-1	2.86e-3	4.71e-3	1.45c-1
128	1.30e-1	7.22e-4	1.53e-3	4.96e-2

Table 3: MDF discretization with stabilizing bubble degrees of freedom on square meshes.

7 Conclusions

We presented a Mimetic Finite Difference method which is an evolution of that of [4]. The method in [4] used a bubble degree of freedom on every mesh edge to achieve stability. In the new method, the bubble degrees of freedom are added instead only where needed, resulting in a smaller algebraic system and potentially in a faster calculations.

In order to investigate where the edge bubbles are needed, we extended the macroelement methodology to polygonal meshes and introduced a new macroelement partition of the mesh. For this partition, we where able to mark a set of edges needing an additional degree of freedom and to prove the stability of the ensuing discrete problem. The set of marked edges is in general significantly compared to the set of all internal mesh edges. For instance, edge bubbles need to be added (roughly) only to every fourth edge of a square mesh, and they are not needed at all on a Voronoi-type mesh.

Finally, we presented a set of numerical tests in complete accordance with the theoretical investigations.

References

[1] B. Andreianov, F. Boyer, and F. Hubert. Discrete duality finite volume schemes for Leray-Lions type elliptic problems on general 2d meshes. *Numer. Methods Partial Differential Equations*, 23(1):145–195, 2007.

[2] I. Babuska. Error bounds for finite element method. *Numer. Math.*, 16:322–333, 1971.

[3] L. Beirão da Veiga. A residual based error estimator for the mimetic finite difference method. *Numer. Math.*, 108(3):387–406, 2008.

[4] L. Beirão da Veiga, V. Gyrya, K. Lipnikov, and G. Manzini. Mimetic finite difference method for the Stokes problem on polygonal meshes. Technical Report LAUR-09-00753, Los Alamos National Laboratory, 2009. Submitted to J. Comp. Phys.

[5] L. Beirão da Veiga, K. Lipnikov, and G. Manzini. Convergence analysis of the high-order mimetic finite difference method. In press on Numer.Math., DOI: 10.1007/s00211-009-0234-6.

[6] L. Beirão da Veiga, K. Lipnikov, and G. Manzini. Convergence of the mimetic finite difference method for the Stokes problem on polyhedral meshes. Technical Report 6PV09/5/0, IMATI-CNR, via Ferrata, 1, 27100 Pavia, Italy, 2009. Submitted for publication.

[7] L. Beirão da Veiga and G. Manzini. An a posteriori error estimator for the mimetic finite difference approximation of elliptic problems. *Int. J. for Numer. Meth. in Engnr.*, 76(11):1696–1723, 2008.

[8] L. Beirão da Veiga and G. Manzini. A higher-order formulation of the mimetic finite difference method. *SIAM Journal on Scientific Computing*, 31(1):732–760, 2008.

[9] M. Berndt, K. Lipnikov, J. D. Moulton, and M. Shashkov. Convergence of mimetic finite difference discretizations of the diffusion equation. *East-West J. Numer. Math.*, 9:253–284, 2001.

[10] M. Berndt, K. Lipnikov, M. Shashkov, M. F. Wheeler, and I. Yotov. Superconvergence of the velocity in mimetic finite difference methods on quadrilaterals. *SIAM J. Numer. Anal.*, 43(4):1728–1749, 2005.

[11] F. Brezzi, A. Buffa, and K. Lipnikov. Mimetic finite differences for elliptic problems. *M2AN Math. Model. Numer. Anal.*, 43:277–295, 2009.

[12] F. Brezzi and M. Fortin. *Mixed and Hybrid Finite Element Methods*. Springer-Verlag, New York, 1991.

[13] F. Brezzi, K. Lipnikov, and M. Shashkov. Convergence of the mimetic finite difference method for diffusion problems on polyhedral meshes. *SIAM J. Numer. Anal.*, 43(5):1872–1896, 2005.

[14] F. Brezzi, K. Lipnikov, M Shashkov, and V. Simoncini. A new discretization methodology for diffusion problems on generalized polyhedral meshes. *Comput. Methods Appl. Mech. Engrg.*, 196:3682–3692, 2007.

[15] F. Brezzi, K. Lipnikov, and V. Simoncini. A family of mimetic finite difference methods on polygonal and polyhedral meshes. *Math. Models Methods Appl. Sci.*, 15(10):1533–1551, 2005.

[16] J. Campbell and M. Shashkov. A tensor artificial viscosity using a mimetic finite difference algorithm. *J. Comput. Phys.*, 172:739–765, 2001.

[17] Y. Coudière and G. Manzini. The discrete duality finite volume method for convection-diffusion problems. Technical Report Tech. Report IMATI-CNR 19PV08/17/0, IMATI-CNR, 2008. To appear in *SIAM Journal on Numerical Analysis*.

[18] K. Domelevo and P. Omnes. A finite volume method for the Laplace equation on almost arbitrary two-dimensional grids. *M2AN Math. Model. Numer. Anal.*, 39(6):1203–1249, 2005.

[19] J. Droniou and R. Eymard. A mixed finite volume scheme for anisotropic diffusion problem on any grid. *Numer. Math.*, 1(105):35–71, 2006.

[20] J. Droniou and R. Eymard. Study of the mixed finite volume method for Stokes and Navier-Stokes equations, 2009. To appear. DOI:10.1002/num.20333.

[21] J. Droniou, R. Eymard, T. Gallouet, and R. Herbin. A unified approach to mimetic finite difference, hybrid finite volume and mixed finite volume method, 2008. Submitted to Math. Model. Methods Appl. Sci.

[22] R. Eymard, T. Gallouet, and R. Herbin. Discretization of heterogeneous and anisotropic diffusion problems on general non-conforming mmeshes. SUSHI: a scheme using stabilization and hybrid interface, 2008. To appear in IMA J. Numer. Anal.

[23] V. Gyrya and K. Lipnikov. High-order mimetic finite difference method for diffusion problems on polygonal meshes. *J. Comput. Phys.*, 227:8841–8854, 2008.

[24] J. Hyman and M. Shashkov. Mimetic discretizations for Maxwell's equations and the equations of magnetic diffusion. *Progress in Electromagnetic Research*, 32:89–121, 2001.

[25] J. Hyman, M. Shashkov, and S. Steinberg. The numerical solution of diffusion problems in strongly heterogeneous non-isotropic materials. *J. Comput. Phys.*, 132:130–148, 1997.

[26] K. Lipnikov, J. Morel, and M. Shashkov. Mimetic finite difference methods for diffusion equations on non-orthogonal non-conformal meshes. *J. Comput. Phys.*, 199, 2004.

[27] K. Lipnikov, M. Shashkov, and I. Yotov. Local flux mimetic finite difference methods. *Numerishe Mathematik*, 112:115–152, 2009.

[28] D.S. Malkus. Eigenproblems associated with the discrete LBB condition for incompressible finite elements. *Int. J. Engr. Sci.*, 19(10):1299–1310, 1981.

[29] L. Margolin, M. Shashkov, and P. Smolarkiewicz. A discrete operator calculus for finite difference approximations. *Comput. Meth. Appl. Mech. Engrg.*, 187:365–383, 2000.

[30] R Stenberg. A technique for analyzing finite-element methods for viscous impompressible flow. *Int J Numer Meth in Fluids*, 11(6):935–948, 1990.